HydroQual, Inc.

Environmental Engineers and Scientists

June 9, 1997

Mr. Douglas Tomchuk
U.S. Environmental Protection Agency
Region II
290 Broadway, 20th Floor
New York, New York 10007-1866

GECO0050

Dear Mr. Tomchuk:

The enclosed report ("Modeling Suspended Load Transport of Non-Cohesive Sediments in the Upper Hudson River") provides a detailed description of the non-cohesive sediment modeling framework that HydroQual has developed at the request of the General Electric Company. This report provides additional information about the Upper Hudson River sediment transport model which was presented at the modeling meeting held in Albany on March 27, 1997. Hopefully, EPA and its contractors will find this report useful in the development and application of an Upper Hudson River sediment transport model. Please contact me if you, or any EPA contractors, have questions or comments regarding this report.

Very truly yours,

HYDROQUAL, INC.

C. Kirk Ziegler

C. Kirk Ziegler, Ph.D.

CKZ:smn
GECO0050\TOMC0609.LTR
Enclosures

cc: William Ports (NYSDEC)
Al DiBernardo (TAMS)
Victor Bierman (Limno Tech)

1 Lethbridge Plaza • Mahwah, NJ • 07430 • 201-529-5151 • FAX 201-529-5728
Mahwah, NJ • Syracuse, NY

General Electric Company
Albany, New York

MODELING SUSPENDED LOAD TRANSPORT OF NON-COHESIVE SEDIMENTS IN THE UPPER HUDSON RIVER

June 1997

Project No: GECO0500

HydroQual, Inc.
Environmental Engineers and Scientists

CONTENTS

FIGURES

SECTION 1

INTRODUCTION

The sediment bed of the Upper Hudson River can generally be separated into two distinct bed types: cohesive and non-cohesive. Cohesive bed deposits are primarily composed of fine-grained sediments, e.g., clay, silt and fine sand, with the median particle diameter (D_{50}) typically being less than 200 μm. The non-cohesive bed is coarser (D_{50} ranging from ~200 μm to over 4,000 μm) and this bed type generally contains significant fractions of non-suspendable sediment, i.e., coarse sand and gravel. In addition, the organic carbon content of cohesive sediment deposits is usually greater than that of the non-cohesive bed.

Analysis of side-scan sonar data collected in the Upper Hudson River shows that the non-cohesive bed comprises at least 50% of the total bed area in each of the three reaches between Fort Edward and Northumberland Dam. Deposition and resuspension from the non-cohesive bed should thus be included in a sediment transport model of the Upper Hudson River because this bed type accounts for a majority of the surface area in the river. A previous study has shown the importance and viability of simulating both cohesive and non-cohesive transport processes in a riverine system (Ziegler and Nisbet, 1994).

The non-cohesive suspended load transport model developed by Ziegler and Nisbet (1994) and applied to the Pawtuxet River, which is located in Rhode Island, has been modified and enhanced for application to the Upper Hudson River. A detailed discussion of the structure of the model, and the formulations used in it, is presented herein. The following section describes the method used to determine resuspension and deposition fluxes at the sediment-water interface for a non-cohesive bed that is composed of a relatively uniform mix of sand particles. Because the non-cohesive sediment bed in the Upper Hudson River is typically graded (heterogeneous) and contains significant fractions of non-suspendable sediments (coarse sand and gravel), the effects of bed armoring must be considered and formulations for simulating non-cohesive bed armoring are presented in Section 3. The fourth section of the report presents a detailed computational procedure for the model and also a discussion on how to calibrate and apply the model.

SECTION 2

NON-COHESIVE SUSPENDED LOAD TRANSPORT MODEL

2.1 INTRODUCTION

Numerous laboratory and field studies have been conducted on the erosion and deposition properties of non-cohesive sediments (e.g., see Vanoni (1975) and van Rijn (1993) for overviews). These investigations have lead to the development of various formulations for quantification of non-cohesive suspended load transport in a riverine system such as the Upper Hudson River. Several investigators have evaluated the accuracy of different quantitative approaches using laboratory and field data (Garcia and Parker, 1991; Voogt et al., 1991; van den Berg and van Gelder, 1993). The results of these investigations have shown that the formulations developed by van Rijn (1984a,b,c) provide one of the best methods for calculating suspended load transport of non-cohesive sediments. The van Rijn equations have also been successfully used in sediment transport modeling studies of riverine (Ziegler and Nisbet, 1994) and estuarine (van Rijn et al., 1990) systems.

Based upon these findings, the van Rijn method for non-cohesive suspended load transport is an appropriate modeling framework for application to the Upper Hudson River. A detailed review of the van Rijn suspended load equations will now be given. For convenience, equation numbers in the original van Rijn publications will be referred to as (VR84a,b,c Eq. _).

An important assumption in the van Rijn procedure is that the sediment bed is composed of relatively homogeneous fine sands so that the following equations apply to the entire sediment bed. As discussed in Section 1, the sediment bed of the Upper Hudson River is heterogeneous, with a significant fraction of the bed being composed of coarse sands ($D > 500\ \mu m$) and gravels ($D > 2000\ \mu m$) which are not transported as suspended load. Modifications that have to be made to the van Rijn equations to account for the effects of non-suspendable bed sediments, i.e., bed armoring, are discussed in Section 3.

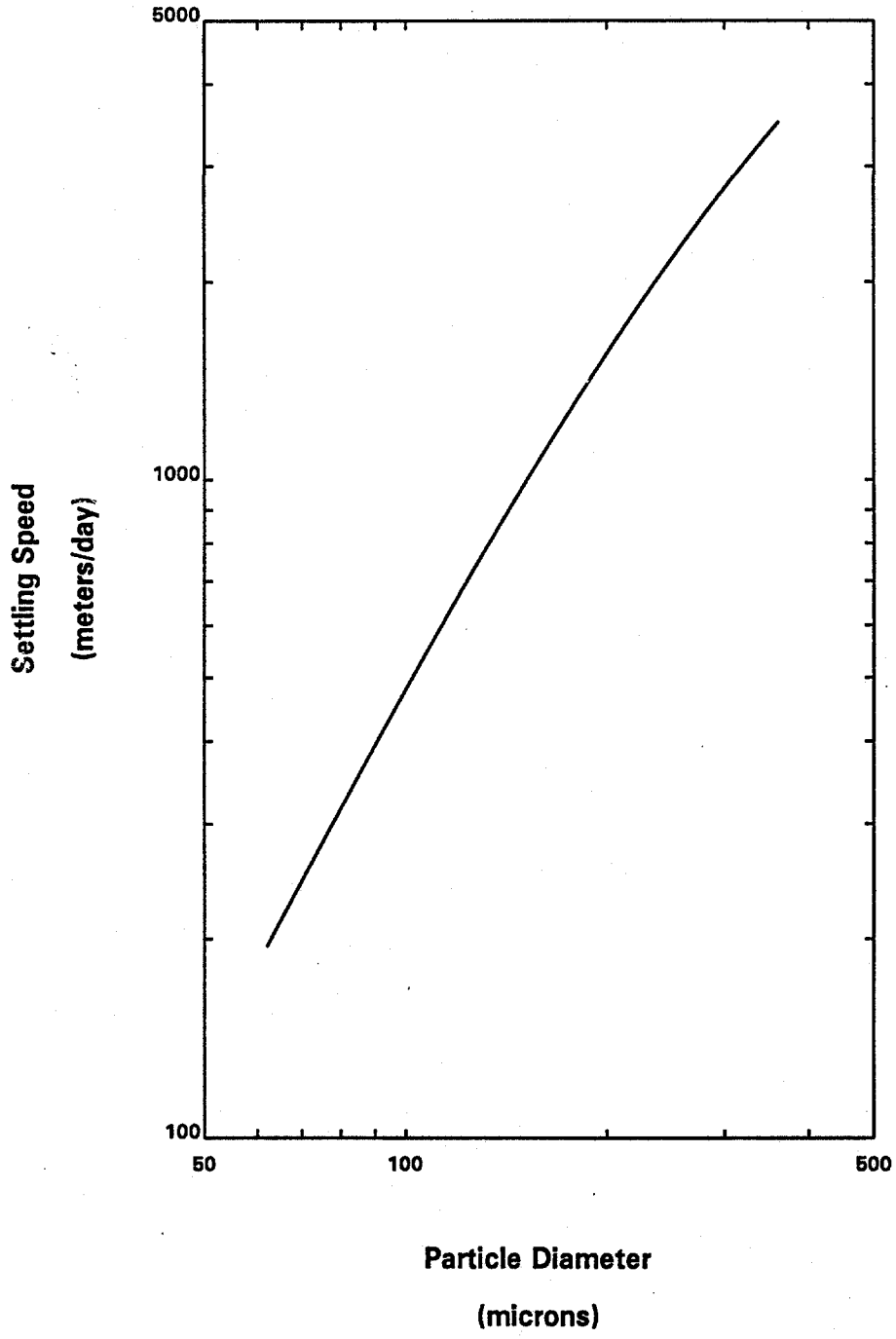

Figure 2-1. Settling speed of sand as function of particle diameter.

2.2 NON-COHESIVE RESUSPENSION

Following the van Rijn method, the equations presented below are used to calculate the suspended load transport rate for a given particle size-class k of suspended sediment, which can be represented by an effective particle diameter (D_k).

The critical bed-shear velocity for initiation of bed load transport ($u_{*,cr}$) is calculated using the Shields criteria (see Figure 1 in VR84a):

$$u_{*,cr} = [(s-1)g\ D_k\ \theta_{cr}]^{1/2} \tag{2-1}$$

where θ_{cr} = critical mobility parameter. For suspendable sands, D_k is less than 500 μm (see Figure 1 in VR84a) and θ_{cr} is calculated as follows:

$$\theta_{cr} = \begin{cases} 0.24\ D_*^{-1} & , \quad D_* \le 4 \\ 0.14\ D_*^{-0.64} & , \quad 4 < D_* \le 10 \\ 0.04\ D_*^{-0.10} & , \quad 10 < D_* \le 20 \end{cases} \tag{2-2}$$

where D_* = non-dimensional particle parameter (VR84b, Eq. 1):

$$D_* = D_k \left[\frac{(s-1)g}{\nu^2}\right]^{1/3} \tag{2-3}$$

where s = specific density of particle (assumed to be 2.65 for sand particles); g = acceleration of gravity; and ν = kinematic viscosity of water.

Experiments on non-cohesive resuspension have shown that the critical bed-shear velocity for initiation of suspension ($u_{*,crs}$) is proportional to the settling speed of particle size-class k ($W_{s,k}$). Laboratory experiments conducted at the Delft Hydraulics Laboratory indicated that (VR84b, Eq. 8 and 9):

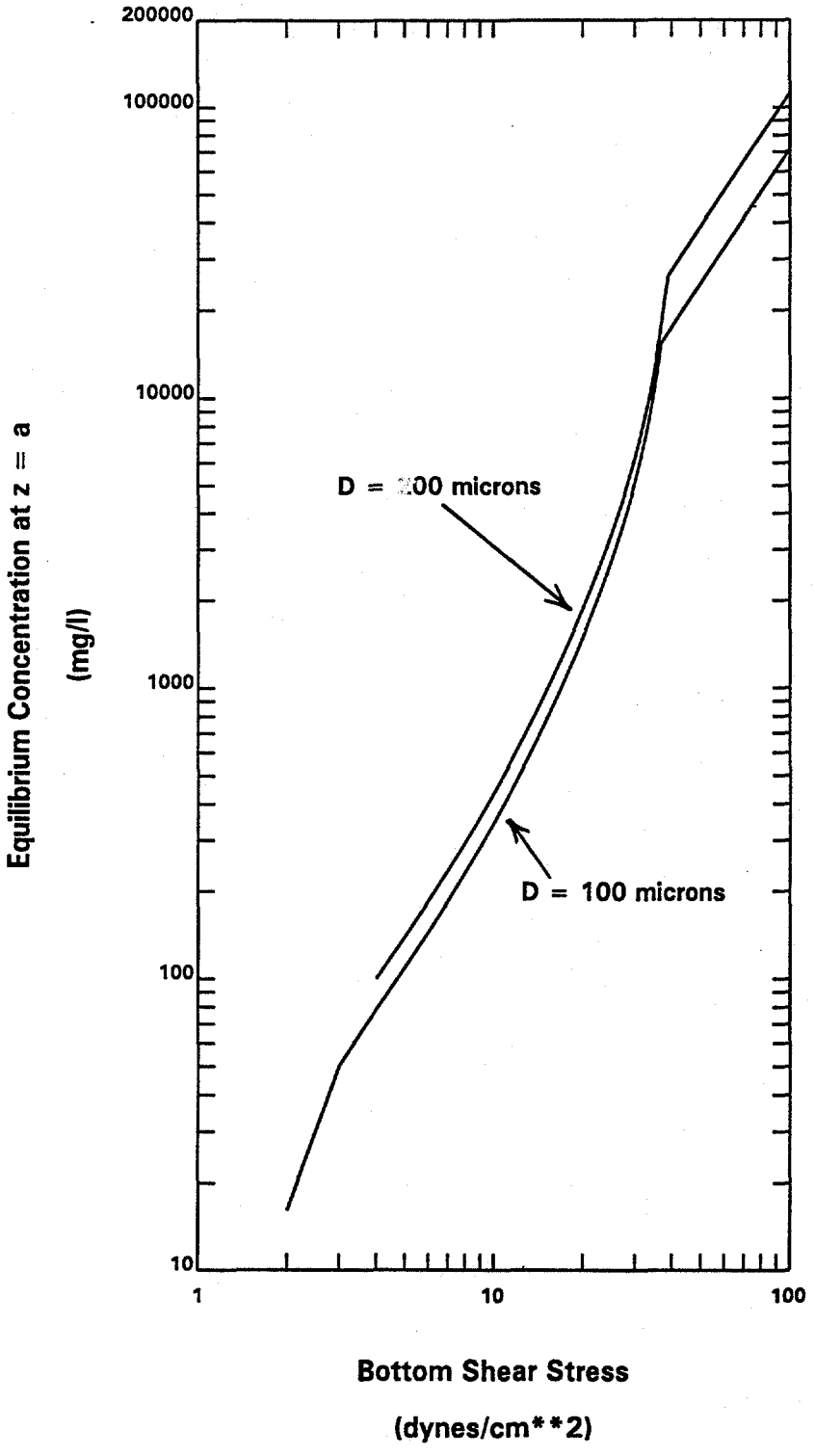

Figure 2-2. Equilibrium concentration at z = a (C_{eq}) as function of bottom shear stress for different particle diameters.

$$u_{*,crs} = \begin{cases} 4\,\dfrac{W_{s,k}}{D_*} & , \quad 1 < D_* \le 10 \\ 0.4\,W_{s,k} & , \quad D_* > 10 \end{cases} \tag{2-4}$$

Note that if $u_{*,crs}$ is less than $u_{*,cr}$, i.e., the critical shear velocity for bed load calculated using Equation (2-1), then $u_{*,crs} = u_{*,cr}$.

The settling speed of a sand particle is related to the particle diameter, representing size-class k, as follows (Cheng, 1997):

$$W_{s,k} = \frac{\nu}{D_k}\left[(25 + 1.2D_*^2)^{1/2} - 5\right]^{1.5} \tag{2-5}$$

The dependence of $W_{s,k}$ on D_k is illustrated in Figure 2-1, which shows that the settling speeds of suspended sand particles (i.e., $62 < D_k < 500$ μm) range from about 2,300 to 59,000 μm/s (~200 to 5,000 m/day).

Once it has been determined that the bottom shear velocity (i.e., bottom shear stress) exceeds the critical values for suspension (i.e., $u_* > u_{*,cr}$ and $u_* > u_{*,crs}$)[1], then an equilibrium reference concentration at a reference height z = a above the sediment bed is calculated (VR84b, Eq. 38):

$$C_{eq} = 0.015\,\frac{D_k\,T^{1.5}}{a\,D_*^{0.3}} \tag{2-6}$$

---

[1]Bottom shear velocity is calculated as

$$u_* = \left(\frac{\tau_b}{\rho}\right)^{1/2}$$

where τ_b = bottom shear stress and ρ = water density.

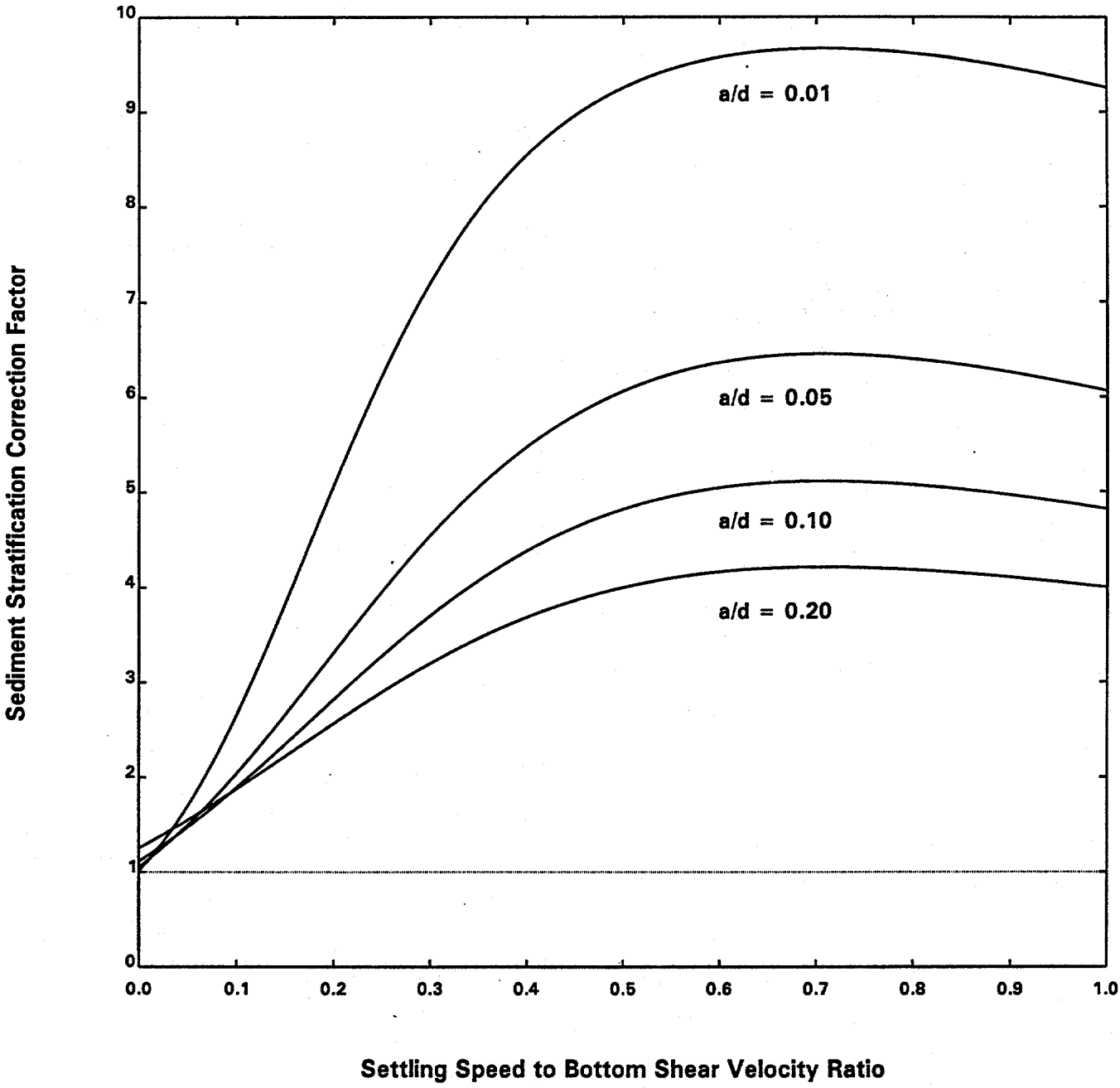

Figure 2-3. Sediment stratification correction factor (Γ) as function of W_s/u_* for various reference heights (normalized with respect to water depth).

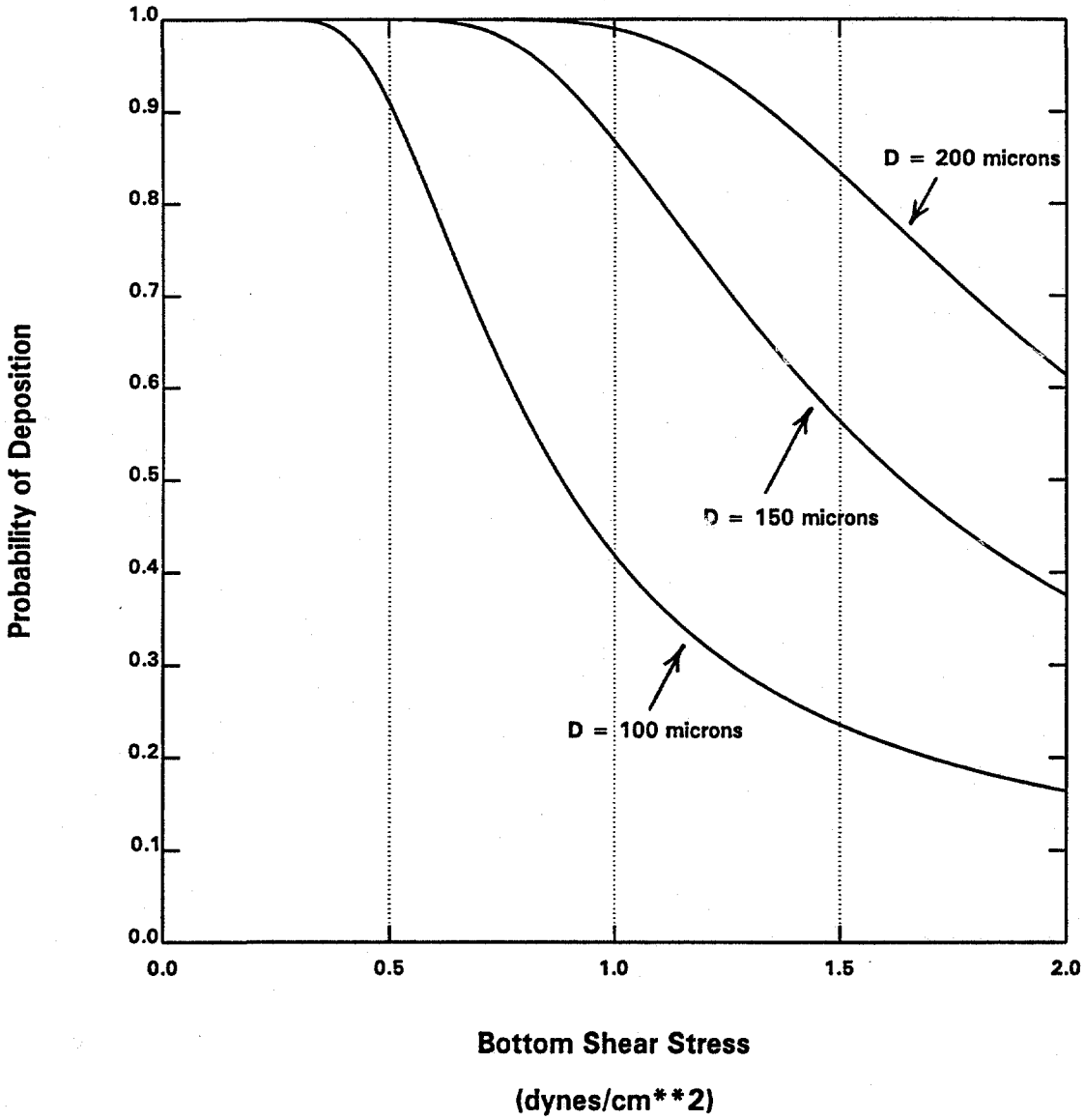

Figure 2-4. Probability of deposition (P_{dep}) of sand as function of bottom shear stress for different particle diameters.

where C_{eq} is a volumetric concentration (i.e., solids volume/unit fluid volume) and T is the transport stage parameter, which is determined using $u_{*,cr}$ (VR84b, Eq.2):

$$T = \left(\frac{u_*}{u_{*,cr}}\right)^2 - 1 \qquad (2\text{-}7)$$

To convert C_{eq} to a mass concentration (i.e., g/cm^3), which is needed for calculating resuspension fluxes, multiply C_{eq} by the sediment particle density (ρ_s). Note that the maximum volumetric concentration ($C_{eq,max}$) is 0.65 or 1.72 g/cm^3 (1,720,000 mg/l) (van Rijn, 1984b). Variation in C_{eq} as a function of τ_b, for different D_k values, is shown on Figure 2-2.

The reference height (a) is given by (VR84b, Eq. 37):

$$a = MAX\ (0.5\ \Delta,\ k_s,\ 0.01d) \qquad (2\text{-}8)$$

where Δ = bed-form height, k_s = equivalent roughness height of Nikuradse and d = local water depth. The bed-form height, where bed-forms are characterized as ripples and dunes, is estimated using (VR84c, Eq. 14):

$$\Delta = 0.11\ d^{0.7}\ D_{50}^{0.3}\ (1 - e^{-0.5T})\ (25 - T) \qquad (2\text{-}9)$$

where D_{50} = median particle diameter of the sediment bed. A plane bed exists when T is greater than 25, i.e., ripples and dunes are washed out and the bed-form height is zero (van Rijn, 1984c).

The resuspension flux is calculated using (van Rijn, 1993):

$$E_{na,k} = -W_{s,k}\ (C_{a,k} - C_{eq}) \qquad (2\text{-}10)$$

where $E_{na,k}$ = net resuspension flux of size-class k for non-armoring sediment bed and $C_{a,k}$ = suspended sediment concentration of size-class k at z=a. A maximum sediment concentration, represented by C_{eq}, can be transported in the water column for a given bed shear velocity (which is equivalent to a certain level of turbulence in the water column). If $C_{a,k} < C_{eq}$, additional sediment can be carried by the flow, so that erosion occurs and $E_{na,k} > 0$. Conversely, if $C_{a,k} > C_{eq}$, the carrying capacity of the water column at a particular bed shear velocity has been exceeded, which means that $E_{na,k} < 0$ and deposition can occur, even though the critical bed shear velocity has been exceeded. Thus, $C_{a,k}$ needs to be calculated before $E_{na,k}$ can be determined, the consequences of which will be discussed in Section 4.

Most sediment transport models applied to riverine systems have used a vertically-averaged approximation of the vertical distribution of sediment in the water column (e.g., Ziegler and Nisbet, 1994). This approach assumes that particles are uniformly distributed throughout the water column, which is a good approximation for cohesive sediments due to their lower settling velocities (ca. 100 μm/s). The high settling speeds of suspended sands cause significant stratification to occur, with order of magnitude increases in concentration typically occurring between the top and bottom of the water column. Thus, simulation of suspended sand transport with a vertically-averaged model necessitates the use of a correction factor (Γ) to account for effects of concentration stratification.

This correction factor will relate the vertically-averaged sediment concentration of size-class k ($C_{m,k}$), which is calculated by the sediment transport model, to $C_{a,k}$ and it is developed as follows. The vertical distribution of non-cohesive sediment in the water column can be calculated using (VR84b, Eq. 19a,b):

$$C_K(z) = \begin{cases} C_{a,k}\left[\left(\frac{a}{d-a}\right)\left(\frac{d}{z} - 1\right)\right]^{\zeta} & , \quad \frac{z}{d} < 0.5 \\ C_{a,k}\left(\frac{a}{d-a}\right)^{\zeta} e^{-4\zeta\left(\frac{z}{d} - 0.5\right)} & , \quad \frac{z}{d} \geq 0.5 \end{cases} \tag{2-11}$$

where z = vertical coordinate (z=0 at sediment-water interface and z=d at water surface) and ζ = suspension parameter (originally denoted as Z in VR84b) defined by (VR84b, Eq. 3):

$$\zeta = \frac{W_{s,k}}{\beta \kappa u_*} \tag{2-12}$$

where κ = von Karman constant (assumed to be 0.4) and the β-factor, which is related to the vertical diffusion of particles, is given by (VR84b, Eq. 22):

$$\beta = 1 + 2\left(\frac{W_{s,k}}{u_*}\right)^2 \quad , \quad 0.1 < \frac{W_{s,k}}{u_*} < 1 \tag{2-13}$$

The vertically-averaged concentration, $C_{m,k}$, is defined as:

$$C_{m,k} = \frac{1}{d}\int_a^d C_k(z)\, dz \tag{2-14}$$

Using Eq. (2-11) in the above integral yields:

$$C_{m,k} = \frac{C_{a,k}}{d}\left(\frac{a}{d-a}\right)^{\zeta}\left\{\int_a^{0.5d}\left(\frac{d}{z}-1\right)^{\zeta} dz + \int_{0.5d}^{d} e^{-4\zeta\left(\frac{z}{d}-0.5\right)} dz\right\} \tag{2-15}$$

The integrals in this equation will be evaluated separately. The first integral does not have a closed form solution. Approximating the solution using the trapezoidal rule (Carnahan et al., 1969) and three segments between z = a and z = 0.5 d, i.e., δz = (0.5 d - a)/3, yields:

$$\int_a^{0.5d}\left(\frac{d}{z}-1\right)^{\zeta} dz = \frac{1}{3}(0.5d-a)\left[0.5\left(\frac{d}{a}-1\right)^{\zeta} + \left(\frac{d}{a+\delta z}-1\right)^{\zeta} + \left(\frac{d}{a+2\delta z}-1\right)^{\zeta} + 0.5\right] \tag{2-16}$$

The second integral has the following solution:

$$\int_{0.5d}^{d} e^{-4\zeta(\frac{z}{d}-0.5)}\, dz = \frac{d}{4\zeta}\,(1 - e^{-2\zeta}) \qquad (2\text{-}17)$$

Inserting Equations (2-16) and (2-17) into Equation (2-15) and solving for C_a produces:

$$C_{a,k} = \Gamma\, C_{m,k} \qquad (2\text{-}18)$$

where:

$$\Gamma = \left(\frac{d}{a}-1\right)^{\zeta}\left\{\frac{1}{4\zeta}\,(1-e^{-2\zeta}) + \frac{1}{3}\left(0.5-\frac{a}{d}\right)\left[0.5\left(\frac{d}{a}-1\right)^{\zeta} + \left(\frac{d}{a+\delta z}-1\right)^{\zeta} + \left(\frac{d}{a+2\delta z}-1\right)^{\zeta} + 0.5\right]\right\}^{-1} \qquad (2\text{-}19)$$

The correction factor, Γ, as a function of $W_{s,k}/u_*$, for various values of a/d, is presented on Figure (2-3).

2.3 NON-COHESIVE DEPOSITION

When the bed-shear velocity is less than the critical value, the resuspension rate is zero and non-cohesive sediments in the water column can be deposited on the sediment bed. The deposition flux for sediments of size-class k (DEP_k) under this condition is:

$$DEP_k = P_{dep}\, W_{s,k}\, C_{a,k} \qquad (2\text{-}20)$$

where P_{dep} = probability of deposition of non-cohesive sediment. The probability of deposition parameter (P_{dep}) accounts for the effects of near-bed turbulence and particle size variations on deposition. In quiescent water, the bottom shear stress will be zero and P_{dep} will equal one. As the bottom shear stress increases, the probability of deposition decreases. The dependence of P_{dep} on bottom shear stress was investigated by Gessler (1967), who determined that P_{dep} could be described by a Gaussian distribution:

$$P_{dep} = \frac{1}{(2\pi)^{1/2}} \int_{-\infty}^{Y} e^{-\frac{1}{2}x^2} dx \qquad (2\text{-}21)$$

where:

$$Y = \frac{1}{\sigma}\left(\frac{\tau_{c,k}}{\tau_b} - 1\right) \qquad (2\text{-}22)$$

and $\tau_{c,k}$ = critical shear stress for size-class k, with

$$\tau_{c,k} = \rho\ [\text{MAX}\ (u_{*,crs}\ ,\ u_{*,cr})]^2 \qquad (2\text{-}23)$$

and σ = standard deviation of the Gaussian distribution for incipient motion. Based upon experimental results, Gessler (1967) determined that σ was equal to 0.57.

An approximation to the probability integral in Equation (2-21), with an error of less than 0.001%, is (Abramowitz and Stegun, 1972):

$$P_{dep}(Y) = 1 - F(Y)\ (0.4362X - 0.1202X^2 + 0.9373X^3), \qquad Y > 0 \qquad (2\text{-}24)$$

where:

$$F(Y) = \frac{1}{(2\pi)^{1/2}} e^{-\frac{1}{2}Y^2} \qquad (2\text{-}25)$$

$$X = (1 + 0.3327Y)^{-1} \qquad (2\text{-}26)$$

For $Y < 0$:

$$P_{dep}(Y) = 1 - P_{dep}(|Y|) \tag{2-27}$$

The dependence of P_{dep} on bottom shear, for different particle sizes, is illustrated on Figure (2-4).

SECTION 3

SIMULATION OF NON-COHESIVE BED ARMORING

3.1 INTRODUCTION

A non-cohesive sediment bed that contains a wide range of particle sizes, from fine sands that are suspendable to coarse sands and gravels that are only transported as bed load, will experience a phenomenon known as bed armoring during a resuspension event. Bed armoring occurs when fine sands are eroded from a heterogeneous sediment bed and the coarser material that cannot be resuspended remains on the bed surface. As the erosion process continues, the suspendable sediments in the near-surface layer, referred to as the active layer, are depleted and a layer of coarse, non-suspendable sediments forms. Continuous depletion of suspendable sediments in the active layer will eventually reduce the erosion rate to zero, at which point the active layer is composed entirely of non-suspendable sediments, and the sediment bed has become armored (Shen and Lu, 1983; Karim and Holly, 1986; Jain and Park, 1989; Rahuel et al., 1989; van Niekerk et al., 1992).

Non-cohesive areas of the sediment bed in the Upper Hudson River typically contain a significant fraction of non-suspendable material. For example, coarse sand and gravel comprises approximately 50% of the non-cohesive bed in the Thompson Island Pool. In addition, an analysis of sediment loading data in the Thompson Island Pool showed that bed armoring occurred on the rising limb of the hydrograph during a high flow event in 1994 (HydroQual, 1997). Thus, the effects of bed armoring must be accounted for in any non-cohesive sediment transport model applied to this reach, or other reaches of the Upper Hudson River. Erosion rates will be significantly overestimated if bed armoring effects are not considered during a sediment transport simulation of a flood event.

3.2 BED ARMORING MODEL

The bed armoring process has been modeled by assuming that the sediment bed is composed of an active layer, which interacts with the water column, and a parent bed layer, which is below the active layer, see Figure 3-1 (Karim and Holly, 1986; van Niekerk et al., 1992). Sediment bed data can be used to determine the initial grain size distribution in the parent bed. The parent bed is aggregated into K size-classes of suspendable sediment (D_k <

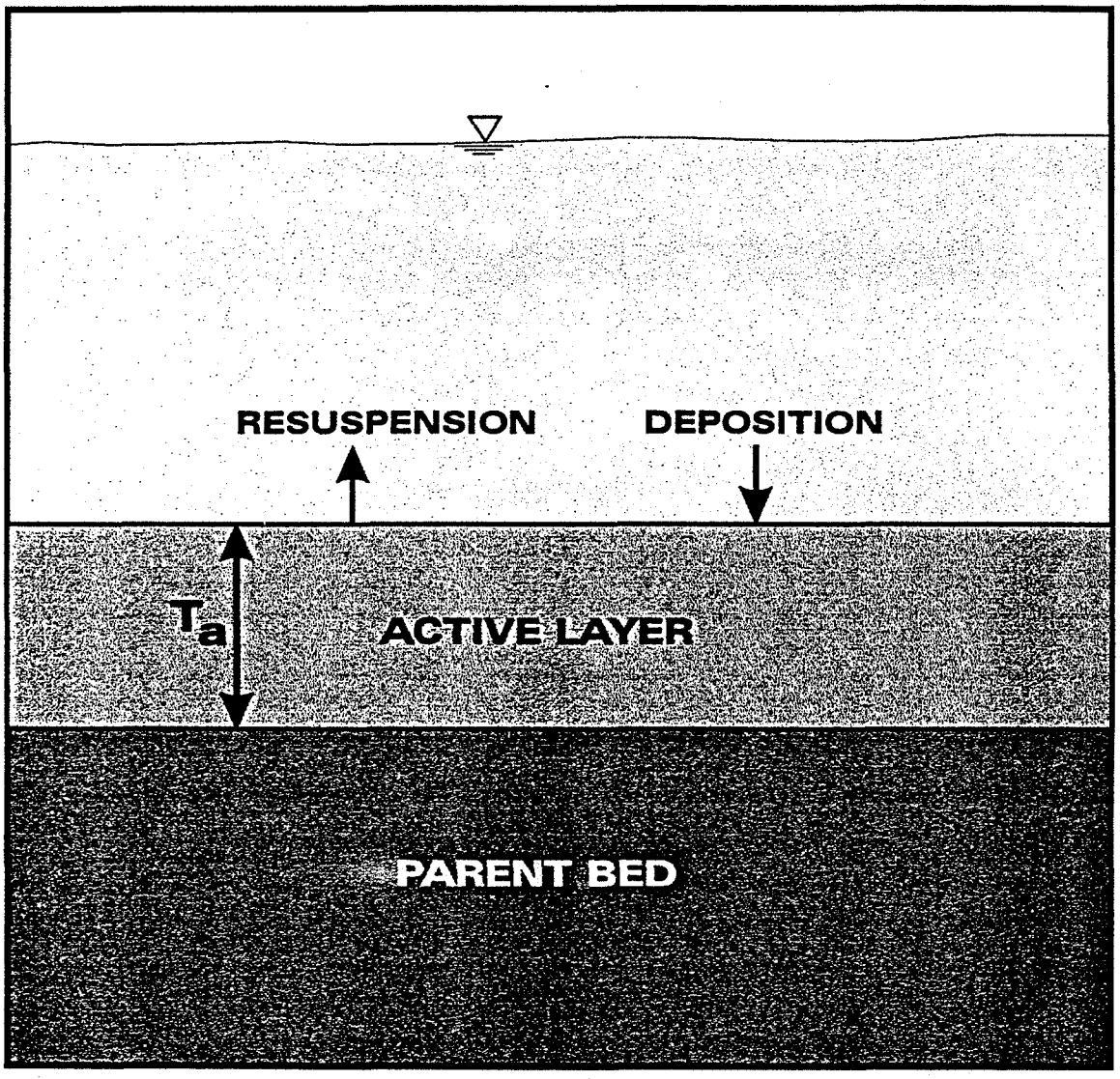

Figure 3-1. Conceptual model of non-cohesive sediment bed.

500 μm, k= 1, K). The fraction of suspendable sediment of size-class k in the parent bed ($f_{p,k}$) is determined from grain size distribution data.

Large, non-suspendable particles in the bed provide voids where smaller, suspendable particles can be shielded from the main flow in the water column. For example, the localized bottom shear stress immediately downstream of a very fine pebble (2,000 μm < D < 4,000 μm) could be much lower than the mean bed shear stress, which might provide a small area in which fine sands (D < 250 μm) could exist without being resuspended. This geometrical effect reduces the suspendable sediment of size-class k below that given by $f_{a,k}$. The reduction factor is referred to as the hiding factor and it is defined as (Karim and Kennedy, 1981; Rahuel et al., 1989):

$$H_k = \left(\frac{D_k}{D_{50}}\right)^m \tag{3-1}$$

where H_k = hiding factor for size-class k and m = site-specific exponent. Karim and Kennedy (1981) set m equal to 0.85, however, Rahuel et al. (1989) stated that the value of m may depend upon local conditions in a particular riverine system. Note that H_k is less than one for an armoring bed.

Interactions between the parent bed, active layer and water column cause the grain size distributions in the parent bed and active layer to change with time. Changes in the active layer grain size distribution control the bed armoring process and, hence, the resuspension flux. The non-cohesive resuspension flux formulation developed in Section 2 assumes that the entire sediment bed is composed of suspendable sediment. Thus, Equation (2-10) must be modified to account for bed armoring effects.

For a non-armoring bed, erosion occurs when the bed shear velocity (u_*) is greater than both the critical shear velocities for bed load ($u_{*,cr}$) and suspended load ($u_{*,crs}$) transport. Both of these critical shear velocities are functions of particle size, see Equations (2-1), (2-4) and (2-5). Bed load transport will be initiated in an armoring bed when the bed shear velocity exceeds the critical shear velocity for the entire bed ($u_{*,cr,bed}$), which is a function of the median particle diameter of the parent bed (D_{50}). The assumption is made that resuspension from an armoring

bed can occur after the initiation of bed load, i.e., $u_* > u_{*,cr,bed}$, provided $u_* > u_{*,crs}$. The value of $u_{*,cr,bed}$ is calculated using Equation (2-1), but with D_{50} replacing D_k.

The fraction of size-class k in the active layer will affect the resuspension rate of that class because sediments are resuspended from the active layer. In addition, the hiding factor will also reduce the resuspension flux, so that (Rahuel et al., 1989):

$$E_k = H_k \, f_{a,k} \, E_{na,k} \tag{3-2}$$

where E_k = net resuspension flux for size-class k and $f_{a,k}$ = fraction of size-class k sediment in the active layer, which will change with time.

Calculating temporal changes of $f_{a,k}$ requires construction of a sediment bed model that tracks compositional changes in the active layer and the parent bed. Size-class k sediment is removed from the active layer at the rate determined by Equation (3-2). The bed model transfers sediment from the parent bed to the active layer at the same rate, but that material has the particle size distribution of the parent bed (Karim and Holly, 1986). This process causes the active layer to become enriched in non-suspendable sediment and eventually it becomes armored; size-class k sediment is resuspended from the active layer at a faster rate than that sediment type is transported into the active layer from the parent bed.

Various expressions have been proposed for the active layer thickness (e.g., Borah et al., 1982; Karim and Holly, 1986; van Niekerk et al., 1992). The Borah et al. (1982) formulation is:

$$T_a = \frac{D_{50}}{(1 - p)\,(1 - \sum f_{a,k})} \tag{3-3}$$

where T_a = active layer thickness, p = bed porosity and $(1 - \Sigma f_{a,k})$ = fraction of the active layer composed of non-suspendable sediment. Initial testing of a Thompson Island Pool sediment transport model has indicated that it may be difficult to adequately calibrate the model using the Borah formulation. These results are probably due to the non-dynamic form of

Equation (3-3), i.e., T_a only depends upon bed properties and it is insensitive to variable hydrodynamic conditions.

An alternative expression for the active layer thickness has been developed by van Niekerk et al. (1992) that is a linear function of the local bottom shear stress. A modified form of their formulation is proposed for application to the Upper Hudson River:

$$T_a = \begin{cases} 2D_{50} & , \ \tau_b < \tau_{c50} \\ 2D_{50}\left[B\left(\frac{\tau_b}{\tau_{c50}}\right) + (1-B)\right] & , \ \tau_b \geq \tau_{c50} \end{cases} \quad (3\text{-}4)$$

where τ_{c50} = critical shear stress for initiation of bed load, based upon parent bed D_{50} and B = adjustable constant. Note that Equation (3-4) reduces to the original van Niekerk et al. (1992) equation when B = 1. A potential advantage of Equation (3-4) is that varying hydrodynamic conditions affect the active layer thickness, with T_a increasing as the current velocity (and τ_b) increases, which causes the amount of sediment that is available for resuspension to increase. The dependence of T_a on τ_b is not well known and the constant (B) in Equation (3-4) can be adjusted during model calibration to account for local conditions.

The approach developed by Karim and Holly (1986) to model changes in the active layer and parent bed composition is used as follows. Sediment volumes are tracked in both layers of the bed model to ensure conservation of mass. The fraction of suspendable sediment, size-class k, in the active layer is defined as:

$$f_{a,k} = \frac{V_{a,k}}{V_{a,tot}} \quad (3\text{-}5)$$

where $V_{a,k}$ = volume of size-class k sediment in the active layer and $V_{a,tot}$ = total volume of sediment in the active layer. The active layer thickness, T_a, is converted to a sediment volume using:

$$V_{a,tot} = (1-p)\ T_a\ A_{ref} \tag{3-6}$$

where A_{ref} = reference area, which is the area of a specific grid element in a numerical model. Similarly, for the parent bed:

$$f_{p,k} = \frac{V_{p,k}}{V_{p,tot}} \tag{3-7}$$

where $f_{p,k}$ = fraction of size-class k sediment in the parent bed layer, $V_{p,k}$ = volume of size-class k sediment in the parent bed layer and $V_{p,tot}$ = total volume of sediment in the parent bed layer and:

$$V_{p,tot} = (1-p)\ T_p\ A_{ref} \tag{3-8}$$

where T_p = thickness of parent bed layer.

Tracking volume changes in the active and parent bed layers with a numerical model is accomplished using the framework proposed by Karim and Holly (1986). It is assumed that the state of the active and parent bed layers are known at some time t^n (i.e., T_a^n, T_p^n, $f_{a,k}^n$, $f_{p,k}^n$, etc. have been calculated or specified). Erosion occurs during the next timestep in the calculation, i.e., $\delta t = t^{n+1} - t^n$, and changes in bed composition need to be determined at t^{n+1}. The mass of size-class k sediment, on a mass/unit area basis, removed from the active layer ($M_{e,k}^{n+1}$) during this timestep is:

$$M_{e,k}^{n+1} = \delta t\ E_k \tag{3-9}$$

where the resuspension rate, E_k, is calculated using Equation (3-2). This mass is converted to a volume for the reference area:

$$V_{e,k}^{n+1} = \frac{A_{ref}}{\rho_s} M_{e,k}^{n+1} \quad (3\text{-}10)$$

where ρ_s = particle density (assumed to be 2.65 g/cm^3 for sand particles).

The total sediment bed thickness (T_{tot}) decreases due to erosion:

$$T_{tot}^{n+1} = T_{tot}^{n} - \frac{\sum V_{e,k}^{n+1}}{(1-p)\, A_{ref}} \quad (3\text{-}11)$$

where $\Sigma\, V_{e,k}{}^{n+1}$ = total eroded volume, i.e., summation for all suspendable size-classes (k = 1, K). Volume changes of size-class k in the active and parent bed layers for a timestep during which erosion occurs also need to account for variations in the active layer thickness (Karim and Holly, 1986). The active layer thickness at t^{n+1} ($T_a{}^{n+1}$) is calculated using Equation (3-4). Thickness of the parent bed at t^{n+1} is given by:

$$T_p^{n+1} = T_{tot}^{n+1} - T_a^{n+1} \quad (3\text{-}12)$$

The above equations are used to calculate volumes of size-class k in the active and parent bed layers at t^{n+1} for increasing active layer thickness ($V_a{}^{n+1} > V_a{}^{n}$):

$$V_{a,k}^{n+1} = V_{a,k}^{n} + f_{p,k}^{n} (V_a^{n+1} - V_a^{n}) - V_{e,k}^{n+1} + f_{p,k}^{n} \sum V_{e,k}^{n+1} \quad (3\text{-}13)$$

$$V_{p,k}^{n+1} = V_{p,k}^{n} - f_{p,k}^{n} (V_a^{n+1} - V_a^{n}) - f_{p,k}^{n} \sum V_{e,k}^{n+1} \quad (3\text{-}14)$$

or decreasing/constant active layer thickness ($V_a{}^{n+1} \leq V_a{}^{n}$):

$$V_{a,k}^{n+1} = V_{a,k}^{n} + f_{a,k}^{n} (V_a^{n+1} - V_a^{n}) - V_{e,k}^{n+1} + f_{p,k}^{n} \sum V_{e,k}^{n+1} \quad (3\text{-}15)$$

$$V_{p,k}^{n+1} = V_{p,k}^{n} - f_{a,k}^{n} (V_a^{n+1} - V_a^{n}) - f_{p,k}^{n} \sum V_{e,k}^{n+1} \quad (3\text{-}16)$$

Equations (3-5) and (3-7) are then used to calculate $f_{a,k}{}^{n+1}$ and $f_{p,k}{}^{n+1}$, respectively, using $V_{a,k}{}^{n+1}$, $V_{p,k}{}^{n+1}$, $V_{a,tot}{}^{n+1}$ and $V_{p,tot}{}^{n+1}$. See Figure 3 of Karim and Holly (1986) for a diagram that illustrates the erosional process and changes in active layer content during a particular timestep.

When depositional conditions occur, as calculated using Equation (2-20), the total depositional volume for each size-class during a timestep is added to the active layer:

$$V_{a,k}^{n+1} = V_{a,k}^{n} + f_{a,k}^{n} \left(V_a^{n+1} - V_a^{n}\right) + \frac{\delta t}{\rho_s} A_{ref} (DEP_k - f_{a,k}^{n} \sum DEP_k) \quad (3\text{-}17)$$

$$V_{p,k}^{n+1} = V_{p,k}^{n} - f_{a,k}^{n} (V_a^{n+1} - V_a^{n}) + \frac{\delta t}{\rho_s} A_{ref} f_{a,k}^{n} \sum DEP_k \quad (3\text{-}18)$$

where the active layer thickness is either decreasing (transition from erosional to depositional conditions) or constant (pure deposition).

SECTION 4

MODEL APPLICATION AND CALIBRATION

4.1 INTRODUCTION

The objective of this section is to suggest procedures that should be followed to ensure that the non-cohesive transport model is used in a consistent and correct manner. First, a step-by-step computational procedure for applying the model is outlined. A discussion on applying the model to the Upper Hudson River, including data requirements and calibration procedures, concludes this section.

4.2 COMPUTATIONAL PROCEDURE

The non-cohesive modeling framework discussed in Sections 2 and 3 is used to calculate resuspension and deposition fluxes across the sediment-water interface. These fluxes are used as a boundary condition in a sediment transport model that transports suspended sediments, of various size-classes, in the water column.

The computational procedure used to calculate sediment flux across the sediment-water interface at a particular location and time (i.e., grid element in a numerical model and at timestep t^{n+1}) assumes that the following information is known at time t^n:

1. Hydrodynamic parameters: u_*, τ_b, d, ν
2. Bed properties: D_{50}, p, ρ_s
3. Active and parent bed composition: $f_{a,k}$, $f_{p,k}$
4. Sediment transport parameter: $C_{m,k}$
5. Numerical parameters: A_{ref}, δt

It is assumed that the sediment bed contains K classes of suspendable sediment, with each size-class k represented by an effective particle diameter, D_k ($D_k < 500\ \mu m$). Note that this necessitates calculating the water column transport of K classes of sediment, with each class having a corresponding vertically-averaged water column concentration at t^n ($C_{m,k}$). Calculating the resuspension or deposition flux of size-class k for a specific location (grid element) at time t^{n+1} proceeds as follows:

1. Calculate D_* for size-class k, Eq. (2-3) using D_k
2. Calculate θ_{cr} for size-class k, Eq. (2-2)
3. Calculate $u_{*,cr}$ for size-class k, Eq. (2-1) using D_k
4. Calculate D_* for parent bed, Eq. (2-3) using D_{50}
5. Calculate θ_{cr} for parent bed, Eq. (2-2)
6. Calculate $u_{*,cr,bed}$ for parent bed, Eq. (2-1) using D_{50}
7. Calculate $W_{s,k}$ for size-class k, Eq. (2-5) using D_k
8. Calculate $u_{*,crs}$ for size-class k, Eq. (2-4)
9. Determine if resuspension or deposition occurs:

   a. If $u_* > MAX(\ u_{*,cr}\ ,\ u_{*,cr,bed}\ ,\ u_{*,crs}\ ) \Rightarrow$ resuspension

   b. If $u_* \leq MAX(\ u_{*,cr}\ ,\ u_{*,cr,bed}\ ,\ u_{*,crs}\ ) \Rightarrow$ deposition

For resuspension conditions:

1. Calculate T for size-class k, Eq. (2-7)
2. Calculate Δ, Eq. (2-9) using D_{50}
3. Calculate a, Eq. (2-8)
4. Calculate C_{eq} for size-class k, Eq. (2-6)
5. Calculate β for size-class k, Eq. (2-13)
6. Calculate ζ for size-class k, Eq. (2-12)
7. Calculate $\delta z = (0.5d - a)/3$
8. Calculate Γ for size-class k, Eq. (2-19)
9. Calculate $C_{a,k}$, Eq. (2-18)

10. Calculate $E_{na,k}$, Eq. (2-10)
11. Calculate H_k, Eq. (3-1)
12. Calculate E_k, Eq. (3-2)
13. Calculate $M_{e,k}^{n+1}$, Eq. (3-9)
14. Calculate $V_{e,k}^{n+1}$, Eq. (3-10)
15. Calculate T_{tot}^{n+1}, Eq. (3-11)
16. Calculate T_a^{n+1}, Eq. (3-4)
17. Calculate T_p^{n+1}, Eq. (3-12)
18. Calculate $V_{a,tot}^{n+1}$, Eq. (3-6)
19. Calculate $V_{p,tot}^{n+1}$, Eq. (3-8)
20. Calculate $V_{a,k}^{n+1}$, Eq. (3-13) or (3-15)
21. Calculate $V_{p,k}^{n+1}$, Eq. (3-14) or (3-16)
22. Calculate $f_{a,k}^{n+1}$, Eq. (3-5)
23. Calculate $f_{p,k}^{n+1}$, Eq. (3-7)

For deposition conditions:

1. Calculate β for size-class k, Eq. (2-13)
2. Calculate ζ for size-class k, Eq. (2-12)
3. Calculate $a = 0.01d$
4. Calculate $\delta z = (0.5d - a)/3$
5. Calculate Γ for size-class k, Eq. (2-19)
6. Calculate $C_{a,k}$, Eq. (2-18)
7. Calculate $\tau_{c,k}$, Eq. (2-23)
8. Calculate Y, Eq. (2-22)
9. Calculate F(Y), Eq. (2-25)
10. Calculate X, Eq. (2-26)
11. Calculate P_{dep}, Eq. (2-24) or (2-27)
12. Calculate DEP_k^{n+1}, Eq. (2-20)
13. Calculate T_{tot}^{n+1}, Eq. (3-11)
14. Calculate T_a^{n+1}, Eq. (3-4)

15. Calculate T_p^{n+1}, Eq. (3-12)
16. Calculate $V_{a,tot}^{n+1}$, Eq. (3-6)
17. Calculate $V_{p,tot}^{n+1}$, Eq. (3-8)
18. Calculate $V_{a,k}^{n+1}$, Eq. (3-17)
19. Calculate $V_{p,k}^{n+1}$, Eq. (3-18)
20. Calculate $f_{a,k}^{n+1}$, Eq. (3-5)
21. Calculate $f_{p,k}^{n+1}$, Eq. (3-7)

4.3 MODEL APPLICATION AND CALIBRATION

Successful application of the non-cohesive suspended load formulations developed in the preceding sections to the Upper Hudson River requires careful development, calibration and validation of the model. First, bed property data in the non-cohesive areas of a particular reach, e.g., Thompson Island Pool, must be analyzed to determine the appropriate bed parameters for use as model input, e.g., D_{50}, p, ρ_s and $f_{p,k}$ for K classes of suspendable sediment. Analysis of non-cohesive bed property data from the Thompson Island Pool indicates the presence of a wide range of D_{50} (from ~200 to 9,000 μm) and $f_{p,k}$ (for 75 μm < D_k < 425 μm, which are fine and medium sands, f_p ranges from 0.06 to 0.85). Judicious examination of the data must be carried out to generate a credible spatial distribution of D_{50} and f_p values throughout this reach.

Once bed property values have been determined, TSS data collected during a high flow event must be used to calibrate the model. The April 1994 high flow event (HydroQual, 1997) yielded a set of TSS data that can be used to calibrate the model in the Thompson Island Pool. The calibration process is important because it demonstrates model accuracy and establishes a certain level of scientific credibility which is necessary before the sediment transport model can be used as a predictive tool.

Use of this model also requires performing time-dependent simulations of water column sediment transport, which can be accomplished using a high flow event for calibration. Time-

dependent calculations are necessary because the resuspension flux, as defined by Equations (2-10) and (3-2), at a particular non-cohesive bed location depends upon the local suspended sediment concentration, as well as various bed properties. Without a time-dependent simulation that calculates suspended sediment concentrations, the non-cohesive resuspension flux cannot be calculated and, hence, scour depths in non-cohesive bed areas cannot be predicted with any confidence.

While the non-cohesive suspended load model developed in this report is based upon formulations presented in peer-reviewed publications, uncertainty exists in some model parameters due to data limitations. Model parameters that cannot be determined using Upper Hudson River data can serve as calibration variables for the model. Calibration of the model in this context means adjustment of various input parameters until the best agreement between model results and data is achieved, e.g., comparison between predicted and observed TSS at one or more locations. However, it must be emphasized that parameter adjustment during calibration cannot be done arbitrarily nor should a large number of parameters be varied in an independent and inconsistent manner. A small number of model parameters, i.e., less than four, need to be adjusted such that the final parameter values are realistic and consistent with data collected from the Upper Hudson River, other riverine systems or laboratory experiments. For the model developed here, the two parameters that are not well known in the Upper Hudson River are: (1) D_k, effective particle diameter of size class k and (2) B, the constant in the active layer thickness formulation expressed in Equation (3-4). These two parameters could be used as the primary calibration parameters for the non-cohesive suspended transport model when it is applied to various reaches in the Upper Hudson River.

Additional testing of the model needs to be done after calibration is completed. This validation is accomplished by simulating other high flow events for which TSS data exist in a particular reach of the Upper Hudson River, e.g., April 1993 and Spring 1997 in the Thompson Island Pool. Model parameters are set at the same values used during calibration and are not adjusted during validation runs; the only model inputs changed are flow rates and solids loadings at the upstream and tributary inflow boundaries.

Confidence in the ability of this model to realistically and accurately simulate non-cohesive suspended load transport, and associated bed armoring, is dependent upon credible calibration and validation results. The uncertainty associated with input and parameter values for this model, or any similar non-cohesive modeling framework, are large enough that successful calibration and validation are necessary before the model can be used as a predictive tool, e.g., simulating the impacts of a 100-year flood. Without direct model-data comparisons, which demonstrate that the model adequately simulates suspended sediment concentrations during at least one high flow event, the model cannot be used as a management tool with any scientific credibility. In other words, an uncalibrated non-cohesive suspended transport model is of questionable value because the uncertainties in the input parameters are so great that an unacceptably low level of confidence will be associated with the model predictions.

Fortunately, adequate data sets exist for the Thompson Island Pool to develop, calibrate and validate the non-cohesive suspended load model described in this report. The model has been applied to this reach of the Upper Hudson River and initial modeling efforts indicate that successful calibration and validation can be achieved using the available data. Thus, this model will be able to be used as a management tool to evaluate the impacts of a 100-year flood or other issues related to sediment transport in the Thompson Island Pool.

SECTION 5

MODEL NOTATION

The following symbols are used in this report:

a = reference height
A_{ref} = reference area
B = constant in Equation (3-4)
$C_{a,k}$ = suspended sediment concentration of size-class k at z = a
$C_{m,k}$ = vertically-averaged suspended sediment concentration of size-class k
C_{eq} = equilibrium concentration at reference height z = a
$C_{eq,max}$ = maximum volumetric concentration (0.65)
$C_k(z)$ = suspended sediment concentration of size-class k at z
d = water depth
D_{50} = median particle diameter of the sediment bed
D_* = non-dimensional particle parameter
D_k = effective particle diameter of size-class k
DEP_k = deposition flux for sediments of size-class k
E_k = net resuspension flux of size-class k for armoring sediment bed
$E_{na,k}$ = net resuspension flux of size-class k for non-armoring sediment bed
$f_{a,k}$ = fraction of size-class k sediment in the active layer
$f_{p,k}$ = fraction of size-class k sediment in the parent bed
$F(Y)$ = probability of deposition parameter
g = acceleration of gravity
H_k = hiding factor for size-class k
k_s = equivalent roughness height of Nikuradse
m = site-specific exponent for hiding factor
$M_{e,k}$ = mass of size-class k sediment eroded from the active layer
p = bed porosity
P_{dep} = probability of deposition of non-cohesive sediment
s = specific density of particle (assumed to be 2.65 for sand)
T = transport stage parameter
T_a = active layer thickness
T_p = parent bed layer thickness

T_{tot} = total sediment bed thickness
u_* = bed shear velocity
$u_{*,cr}$ = critical bed-shear velocity for initiation of bed load transport (based on D_k)
$u_{*,cr,bed}$ = critical bed-shear velocity for initiation of bed load transport (based on D_{50})
$u_{*,crs}$ = critical bed-shear velocity for initiation of suspension
$V_{a,k}$ = volume of size-class k sediment in the active layer
$V_{a,tot}$ = total volume of sediment in the active layer
$V_{e,k}$ = volume of size-class k sediment eroded from the active layer
$V_{p,k}$ = volume of size-class k sediment in the parent bed
$V_{p,tot}$ = total volume of sediment in the parent bed
$W_{s,k}$ = settling speed of particle size-class k
X = probability of deposition parameter
Y = probability of deposition parameter
z = vertical coordinate (z = 0 at sediment-water interface and z = d at surface)
β = β-factor
Γ = sediment stratification correction factor
δt = $t^{n+1} - t^n$ (timestep in numerical model)
δz = (0.5d - a)/3
Δ = bed form height
ζ = suspension parameter (originally denoted as Z in VR84b)
θ_{cr} = critical mobility parameter
κ = von Karman constant (0.4)
ν = kinematic viscosity of water
ρ = water density
ρ_s = sediment particle density (2.65 g/cm^3)
σ = standard deviation of the Gaussian distribution for incipient motion (0.57)
τ_b = bottom shear stress
$\tau_{c,k}$ = critical shear stress for size-class k
τ_{c50} = critical shear stress based on D_{50}

SECTION 6

REFERENCES

Abramowitz, M. and Stegun, I.A., 1972. *Handbook of Mathematical Functions*, National Bureau of Standards, Applied Mathematics Series 55, Washington, D.C.

Borah, D.K., Alonso, C.V. and Prasad, S.N., 1982. Routing Graded Sediments in Streams: Formulations, *J. Hydr. Engrg.*, ASCE, 108(12):1486-1503.

Carnahan, B., Luther, H.A. and Wilkes, J.O., 1969. *Applied Numerical Methods*, John Wiley & Sons, New York.

Cheng, N.S., 1997. Simplified Settling Velocity Formula for Sediment Particle, *J. Hydr. Engrg.*, ASCE, 123(2):149-152.

Garcia, M. and Parker, G., 1991. Entrainment of Bed Sediment Into Suspension, *J. Hydr. Engrg.*, ASCE, 117(4):414-435.

Gessler, J., 1967. *The Beginning of Bedload Movement of Mixtures Investigated as Natural Armoring in Channels*, W.M. Keck Laboratory of Hydraulics and Water Resources, California Institute of Technology, Translation T-5.

HydroQual, 1997. *Analysis of Sediment Loading to the Upper Hudson River During the April 1994 High Flow Event*, HydroQual report.

Jain, S.C., and Park, I., 1989. Guide for Estimating Riverbed Degradation, *J. Hydr. Engrg.*, ASCE, 115(3):356-366.

Karim, M.F. and Holly, F.M., 1986. Armoring and Sorting Simulation in Alluvial Rivers, *J. Hydr. Engrg.*, ASCE, 112(8):705-715.

Karim, M.F. and Kennedy, J.F., 1981. *Computer-Based Predictors for Sediment Discharge and Friction Factor of Alluvial Streams,* IIHR Report No. 242, Univ. of Iowa, Iowa City, Iowa.

Rahuel, J.L., Holly, F.M., Chollet, J.P., Belleudy, P.J. and Yang, G., 1989. Modeling of Riverbed Evolution for Bedload Sediment Mixtures, *J. Hydr. Engrg.*, ASCE, 115(11):1521-1542.

Shen, H.W. and Lu, J.Y., 1983. Development and Prediction of Bed Armoring, *J. Hydr. Engrg.*, ASCE, 109(4):611-629.

van den Berg, J.H. and van Gelder, A., 1993. Prediction of Suspended Bed Material Transport in Flows Over Silt and Very Fine Sand, *Water Resour. Res.,* 29(5):1392-1404.

van Niekerk, A., Vogel, K.R., Slingerland, R.L. and Bridge, J.S., 1992. Routing of Heterogeneous Sediments Over Movable Bed: Model Development, *J. Hydr. Engrg.*, ASCE, 118(2):246-279.

Vanoni, V.A., 1975. *Sedimentation Engineering*, ASCE, New York.

van Rijn, L.C., 1984a. Sediment Transport, Part I: Bed Load Transport, *J. Hydr. Engrg.*, ASCE, 110(10):1431-1456.

van Rijn, L.C., 1984b. Sediment Transport, Part II: Suspended Load Transport, *J. Hydr. Engrg.*, ASCE, 110(11): 1612-1638.

van Rijn, L.C., 1984c. Sediment Transport, Part III: Bed Forms and Alluvial Roughness, *J. Hydr. Engrg.*, ASCE, 110(12): 1732-1754.

van Rijn, L.C., 1993. *Principles of Sediment Transport in Rivers, Estuaries and Coastal Seas*, Aqua Publications, The Netherlands.

van Rijn, L.C., van Rossum, H. and Termes, P., 1990. Field Verification of 2-D and 3-D Suspended-Sediment Models, *J. Hydr. Engrg.*, ASCE, 116(10): 1270-1288.

Voogt, L., van Rijn, L.C. and van den Berg, J.H., 1991. Sediment Transport of Fine Sands at High Velocities, *J. Hydr. Engrg.*, ASCE, 117(7): 869-890.

Ziegler, C.K. and Nisbet, B., 1994. Fine-Grained Sediment Transport in Pawtuxet River, Rhode Island, *J. Hydr. Engrg.*, ASCE, 120(5): 561-576.